The VIMOS VLT Deep Survey - The evolution of galaxy clustering to z=2 from first epoch observations

O. Le Fevre, L. Guzzo, B. Meneux, A. Pollo, A. Cappi, S. Colombi, A. Iovino, Christian Marinoni, H. J. Mccracken, R. Scaramella, et al.

A&A 439, 877–885 (2005)
DOI: 10.1051/0004-6361:20041962

Astronomy & Astrophysics

The VIMOS VLT deep survey

The evolution of galaxy clustering to $z \simeq 2$ from first epoch observations⋆

O. Le Fèvre[1], L. Guzzo[2], B. Meneux[1], A. Pollo[2], A. Cappi[3], S. Colombi[9], A. Iovino[2], C. Marinoni[1,2], H. J. McCracken[9,12], R. Scaramella[7], D. Bottini[4], B. Garilli[4], V. Le Brun[1], D. Maccagni[4], J. P. Picat[5], M. Scodeggio[4], L. Tresse[1], G. Vettolani[6], A. Zanichelli[6], C. Adami[1], M. Arnaboldi[11], S. Arnouts[1], S. Bardelli[3], J. Blaizot[1], M. Bolzonella[8], S. Charlot[9,10], P. Ciliegi[6], T. Contini[5], S. Foucaud[4], P. Franzetti[4], I. Gavignaud[5,13], O. Ilbert[1,3], B. Marano[8], G. Mathez[5], A. Mazure[1], R. Merighi[3], S. Paltani[1], R. Pellò[5], L. Pozzetti[3], M. Radovich[11], G. Zamorani[3], E. Zucca[3], M. Bondi[6], A. Bongiorno[8], G. Busarello[11], F. Lamareille[5], Y. Mellier[9,12], P. Merluzzi[11], V. Ripepi[11], and D. Rizzo[5,2]

[1] Laboratoire d'Astrophysique de Marseille, UMR 6110 CNRS-Université de Provence, Traverse du Siphon, BP 8, 13012 Marseille, France
e-mail: olivier.lefevre@oamp.fr
[2] INAF – Osservatorio Astronomico di Brera, via Brera 28, 20121 Milan, Italy
[3] INAF – Osservatorio Astronomico di Bologna, via Ranzani 1, 40127 Bologna, Italy
[4] INAF – IASF, via Bassini, 15, 20133 Milano, Italy
[5] Laboratoire d'Astrophysique de l'Observatoire Midi-Pyrénées, UMR 5572, 14 Av. Ed. Belin, 31400 Toulouse, France
[6] INAF – Istituto di Radio-Astronomia, via Gobetti 101, 40129 Bologna, Italy
[7] INAF – Osservatorio Astronomico di Roma, Italy
[8] Dipartimento di Astronomia, Università di Bologna, via Ranzani 1, 40127 Bologna, Italy
[9] Institut d'Astrophysique de Paris, UMR 7095, 98bis Bd. Arago, 75014 Paris, France
[10] Max-Planck-Institut für Astrophysik, 85741 Garching, Germany
[11] INAF – Osservatorio Astronomico di Capodimonte, via Moiariello 16, 80131 Napoli, Italy
[12] Observatoire de Paris, LERMA, UMR 8112, 61 Av. de l'Observatoire, 75014 Paris, France
[13] European Southern Observatory, Karl Schwarzschild Str. 2, 85748 Garching bei München, Germany

Received 6 September 2004 / Accepted 11 April 2005

Abstract. This paper presents the evolution of the clustering of the main population of galaxies from $z \simeq 2$ to $z = 0.2$, from the first epoch VIMOS VLT Deep Survey (VVDS), a magnitude limited sample with $17.5 \leq I_{AB} \leq 24$. The sample allows a direct estimate of evolution *from within the same survey* over the time base sampled. We have computed the correlation functions $\xi(r_\mathrm{p}, \pi)$ and $w_\mathrm{p}(r_\mathrm{p})$, and the correlation length $r_0(z)$, for the VVDS-02h and VVDS-CDFS fields, for a total of 7155 galaxies in a 0.61 deg^2 area. We find that the correlation length in this sample slightly increases from $z = 0.5$ to $z = 1.1$, with $r_0(z) = 2.2$–$2.9\ h^{-1}$ Mpc (comoving), for galaxies comparable in luminosity to the local 2dFGRS and SDSS samples, indicating that the amplitude of the correlation function was $\simeq$2.5 times lower at $z \simeq 1$ than observed locally. The correlation length in our lowest redshift bin $z = [0.2,\ 0.5]$ is $r_0 = 2.2\ h^{-1}$ Mpc, lower than for any other population at the same redshift, indicating the low clustering of very low luminosity galaxies, 1.5 mag fainter than in the 2dFGRS or SDSS. The correlation length increases to $r_0 \sim 3.6\ h^{-1}$ Mpc at higher redshifts $z = [1.3,\ 2.1]$, as we are observing increasingly brighter galaxies, comparable to galaxies with $M_{B_{AB}} = -20.5$ locally. We compare our measurement to the DEEP2 measurements in the range $z = [0.7,\ 1.35]$ (Coil et al. 2004, ApJ, in press) and find comparable results when applying the same magnitude and color selection criteria as in their survey. The slowly varying clustering of VVDS galaxies as redshift increases is markedly different from the predicted evolution of the clustering of dark matter, indicating that bright galaxies traced higher density peaks when the large scale structures were emerging from the dark matter distribution 9–10 billion years ago, being supporting evidence for a strong evolution of the galaxy vs. dark matter bias.

Key words. surveys – galaxies: evolution – cosmology: large scale structure of Universe

⋆ Based on data obtained with the European Southern Observatory Very Large Telescope, Paranal, Chile, program 070.A-9007(A), and on data obtained at the Canada-France-Hawaii Telescope, operated by the CNRS of France, CNRC in Canada and the University of Hawaii.

1. Introduction

The evolution of the clustering of galaxies is a key diagnostic element to test the evolution of the universe, allowing direct comparison between observations and theory. In the current paradigm of galaxy formation and evolution, dark matter halos that contain galaxies are expected to merge and grow under the action of gravity. This translates into a continuous evolution of the correlation function $\xi(r, z)$ of dark matter halos, now quite well understood from extensive high resolution numerical simulations (see Weinberg et al. 2004; Benson et al. 2001; Somerville et al. 2001; Kauffmann et al. 1999). As a direct measurement of the space distribution of dark matter halos is not yet feasible, we are compelled to use galaxies as indirect tracers of the dark matter. Unfortunately, as galaxies are complex physical systems, their relationship to the underlying mass, the "bias", is difficult to estimate. As galaxies and dark matter evolve, the bias may evolve and relating the measurements of galaxy clustering to the evolution of the total mass is not easy, with the bias shown to depend upon galaxy type, luminosity and local environment (Norberg et al. 2002).

The most straigthforward indicator of galaxy clustering is the correlation function $\xi(r)$, representing the excess probability over random of finding a galaxy in a given volume, at a fixed distance from another galaxy. The shape and amplitude of the galaxy correlation function at the current epoch is now established to high accuracy. $\xi(r)$ is well described by a power law $\xi(r) = (r/r_0)^{-\gamma}$ over scales 0.1−10 h^{-1} Mpc (Davis & Peebles 1983; Hawkins et al. 2003; Zehavi et al. 2004), with a more refined modelling requiring some extra power over this shape for separations larger than 2–3 h^{-1} Mpc (Guzzo et al. 1991; Zehavi et al. 2004), a feature possibly encoding information on the relation between galaxies and their host dark-matter halos. The local clustering measurements have shown that the correlation length r_0 increases from late types to early type galaxies, from low luminosity to high luminosity and from low to high galaxy density environments (see Giovanelli et al. 1986; Benoist et al. 1996; Guzzo et al. 1997; Norberg et al. 2001), with luminosity being the dominant effect (Norberg et al. 2002). The most recent estimates of the correlation length from the 2dFGRS and SDSS vary from $r_0 = 3$ for late type star-forming galaxies in low density environments to $r_0 = 5$−6 for galaxies with $M_* = -19.5$, with the clustering amplitude reaching $r_0 = 7.5\ h^{-1}$ Mpc for galaxies four times L_*.

At higher redshifts the situation is less clear. Analysis of the projected angular correlation function favors a stable clustering (Postman et al. 1998; Roche et al. 1999; McCracken et al. 2001; Cabanac et al. 2000) but it requires a priori knowledge of the redshift distribution of the galaxy population sampled. A variety of results have been obtained from smaller spectroscopic samples, with comoving correlation lengths r_0 in the range 2−5 h^{-1} Mpc at $z \sim 0.5$ (Le Fèvre et al. 1996; Small et al. 1999; Shepherd et al. 2001; Carlberg et al. 1999) and $r_0 = 3$−5 h^{-1} Mpc at $z \sim 3$ (Giavalisco et al. 1998; Foucaud et al. 2003). Recently, first results from the DEEP2 survey have been presented, indicating a correlation length $r_0 = 3.53 \pm 0.81\ h^{-1}$ Mpc in $z = [0.7,\ 0.9]$, and $r_0 = 3.12 \pm 0.72\ h^{-1}$ Mpc in $z = [0.9,\ 1.35]$ (Coil et al. 2004). The main difficulty in interpreting these results in terms of evolution of the clustering is to relate the population of galaxies observed at a given redshift to a lower redshift population of "descendants", identified from a well-defined selection function enabling comparisons. Some of these surveys are targeted to specific classes of galaxies, pre-selected via photometric methods, whose relation to the global population is not obvious. The most notable example is represented by galaxies selected via the Lyman-break technique around $z \sim 3$ and $z \sim 4$ (Steidel et al. 1998), which display a clustering strength similar to present-day normal galaxies and therefore represent a very *biased* population, possibly the precursors of giant cluster ellipticals (Governato et al. 1998).

On the other hand, even when selecting purely magnitude-limited samples, one cannot avoid being affected by the complex dependence of clustering on morphology and luminosity evidenced by the wide range of correlation lengths measured in the local Universe, and its evolution as a function of redshift. One needs to observe samples at increasingly high redshifts with the same luminosities, colors (type) and local environments in order to derive the evolution of the clustering of galaxies and hence attempt to derive how the correlation properties of the mass evolve. At high redshifts, the natural observational bias is to sample increasingly brighter and more actively star forming galaxies, which may have a direct impact on our current vision of the evolution.

Finally, high-redshift samples of spectroscopically measured galaxies have been inevitably limited so far to relatively bright objects in small areas on the sky, which contributes to increase the scatter between independent measurements, further complicating their interpretation.

In this paper we present the first attempt to measure the evolution of the clustering in a consistant way accross the redshift range $0.2 < z \leq 2.1$, using 7155 galaxies from the VIMOS VLT Deep Survey (VVDS) over more than 0.61 deg^2. The VVDS is designed to sample the high redshift population of galaxies in the most unbiased way possible, using a simple magnitude selection in the range $17.5 \leq I_{AB} \leq 24$, using several independant fields up to 4 deg^2 each (Le Fèvre et al. 2005). This analysis uses the high-quality First Epoch VVDS sample, which includes 6117 galaxy redshifts in the VVDS-02h (Le Fèvre et al. 2005) and another 1368 galaxies in the VVDS-CDFS (Le Fèvre et al. 2004b) field. We have measured the redshift-space correlation function $\xi(r_\mathrm{p}, \pi)$, and computed the projected function $w_\mathrm{p}(r_\mathrm{p})$, to recover the value of the galaxy correlation length $r_0(z)$ up to $z \simeq 2$, therefore tracing the evolution of the clustering over more than 10 Gy, or 70% of the current age of the universe.

In Sect. 2 we recall the properties of the VVDS First Epoch sample. In Sect. 3, we describe how the correlation function has been computed, referring in large part to the accompanying paper by Pollo et al. (2005) which describes all the methods set up to validate the measurements and compute the errors. In Sect. 4, we present the results in terms of the evolution of $r_0(z)$, and we compare our results to previous measurements where possible. In Sect. 5, we discuss the evolution of the clustering of the global population of galaxies from $z \simeq 2$, before concluding in Sect. 6.

This paper is the first in a series of papers to study the clustering of galaxies at high redshift from the VVDS first epoch data. Guzzo et al. (2005, in prep.) will present the clustering evolution from volume limited samples and infer the dependence of clustering upon luminosity; Meneux et al. (2005, in prep.) will present the differences in clustering observed as a function of galaxy type and its evolution and Pollo et al. (2005, in prep.) will investigate the dependence and evolution of clustering as a function of the local environment. Marinoni et al. (2005) and Le Fèvre et al. (2005, in prep.) will look at the evolution of the galaxy – dark matter bias, and subsequent papers will study the clustering from the redshift population $2 \leq z \leq 5$.

We have used a Concordance Cosmology with $\Omega_{\rm m} = 0.3$, and $\Omega_\Lambda = 0.7$ throughout this paper. The Hubble constant is normally parameterized via $h = H_0/100$, to ease comparison to previous works, while a value $H_0 = 70$ km s^{-1} Mpc^{-1} has been used when computing absolute magnitudes. All correlation length values are quoted in comoving coordinates.

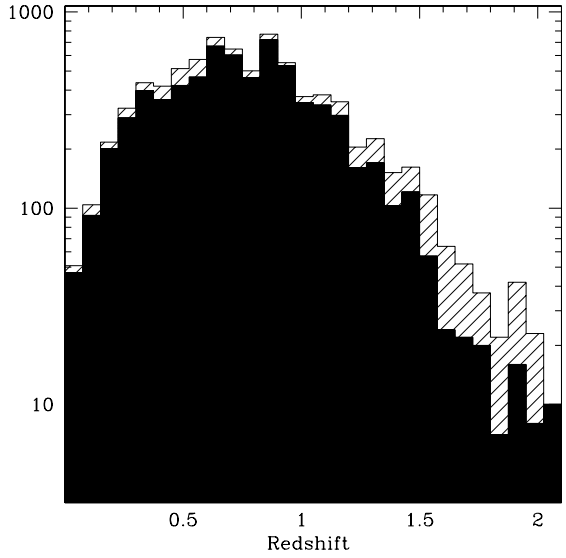

Fig. 1. The redshift distribution in the VVDS-02h field. The filled histogram contains 6137 galaxies with quality flag ≥2, and another 1093 galaxies with quality flag = 1 (open dashed histogram), in the redshift range $z = [0.2,\ 2.1]$.

2. VVDS first epoch data

2.1. The sample

The VVDS-Deep sample is stricly selected in magnitude in the range $17.5 \leq I_{AB} \leq 24$, from a complete deep photometric survey (Le Fèvre et al. 2004a; McCracken et al. 2003) without any color or shape selection (Le Fèvre et al. 2004b). We have analysed two fields, the VVDS-02h and the VVDS-CDFS. Over the ∼9600 redshifts measured in these two fields, we have used in the following analysis only objects with a redshift confidence level higher than or equal to ≃80% (quality flags 2 to 9 as defined in Le Fèvre et al. 2004b), excluding QSOs. We will only mention briefly below the effect on measured correlations of relaxing the quality threshold, including the poorest redshift measurements (flag 1). The complete sample analysed concerns a total of 7155 galaxies in 2203 arcmin^2, with 6137 galaxies in the 1750 arcmin^2 VVDS-02h field with $0.2 \leq z \leq 2.1$, and 1038 galaxies in the 453 arcmin^2 VVDS-CDFS (Chandra Deep Field South, Giacconi et al. 2002) area with $0.4 \leq z \leq 1.5$. The accuracy of the redshift measurements is ≃275 km s^{-1} (Le Fèvre et al. 2004a). The distribution of redshifts for the VVDS-02h field is presented in Fig. 1. The redshift distribution peaks at $z \simeq 0.8$, and there are 300 galaxies with $1.3 \leq z \leq 1.5$, and 132 galaxies with $1.5 \leq z \leq 2.1$.

2.2. The galaxy population mix

We have split the sample into 6 redshift bins, as described in Table 1. The rest frame $B - I_{AB}(0)$ color and absolute magnitude $M_{B_{AB}}$ distribution within each bin is shown in Fig. 2, from $z = 0.2$ to $z = 2.1$, and the mean values are reported in Table 1. $B - I_{AB}(0)$ and $M_{B_{AB}}$ have been computed using template fitting of the photometric spectral energy distribution in B, V, R, and I bands, to derive the k(z) corrections (see Ilbert et al. 2005, for details).

Up to redshift $z = 1.3$, the $B - I_{AB}(0)$ color distribution stays quite similar with increasing redshift, from blue star forming $B - I_{AB}(0) = 0$ to red $B - I_{AB}(0) \sim 3$, while for $1.3 < z \leq 2.1$, the reddest $B - I_{AB}(0) \geq 2.5$ galaxies, if present, are not observed. The magnitude selection of the VVDS-Deep, therefore, allows us to sample the global population of galaxies, for all galaxy types from late to early types, up to $z \sim 1.3$, while for $z > 1.3$, as we are selecting galaxies from their UV rest frame continuum at these redshifts, the VVDS is increasingly biased towards late-type, higher star-forming galaxies. We therefore expect that in the farthest redshift bin, the clustering measurement in the VVDS is the result of the effects of looking at intrinsicaly more luminous and more actively star forming galaxies.

The range of absolute $M_{B_{AB}}$ magnitudes sampled is quite large, and changes strongly with redshift as shown in Fig. 2. While at redshift $z \sim 0.5$, the absolute magnitude range sampled is $-22 \leq M_{B_{AB}} \leq -16$, only bright galaxies with $M_{B_{AB}} \leq -20$ are sampled at $z > 1.3$. The absolute luminosity of galaxies in the VVDS is shown to increase as redshift increases, as computed from the Luminosity Function (Ilbert et al. 2005). If one assumes a pure luminosity evolution, galaxies observed at high redshift are expected to have faded to fainter absolute magnitudes at the present time, by as much as $M_B = 1.5$ to 2 mag. This should be taken into account when comparing the clustering of the high redshift population to local populations.

The consequences on the correlation function measurements of the change in the population sampled as a function of redshift are discussed in Sect. 5.

3. Computing the real-space correlation and correlation length $r_0(z)$

The methods applied on the VVDS first epoch data to derive the real space correlation parameters are described extensively in the accompanying paper by Pollo et al. (2005). We summarize below the main elements of this method.

Table 1. Measurements of the correlation length $r_0(z)$ and the correlation function slope $\gamma(z)$. The associated 1σ errors are reported. r_0 values are computed both with letting γ free, and setting γ to the mean 1.78 in the range $z = [0.2,\ 1.3]$ in the VVDS-F02 and VVDS-CDFS. To compare to the DEEP2 measurements of Coil et al. (2004), we have set $\gamma = 1.66$ for the VVDS-F02-DEEP2 in $z = [0.7,\ 0.9]$ and $z = [0.9,\ 1.35]$, and $\gamma = 1.68$ for the VVDS-F02-DEEP2 in $z = [0.7,\ 1.35]$. The redshift range, number of galaxies used, mean absolute magnitude $M_{B_{AB}}$ and rest frame color $B - I_{AB}(z = 0)$, are indicated for each subsample.

Field	Redshift range	$N_{\rm gal}$	mean $M_{B_{AB}}$	mean $B - I_{AB}(z = 0)$	$r_0(z)$ h^{-1} Mpc	γ	$r_0(z)$ (fixed γ)
VVDS-02h	[0.2−0.5]	1258	−17.57	1.34	$2.23^{+0.46}_{-0.51}$	$1.67^{+0.17}_{-0.11}$	$2.27^{+0.47}_{-0.52}$
VVDS-02h	[0.5−0.7]	1443	−18.68	1.28	$2.69^{+0.53}_{-0.59}$	$1.71^{+0.18}_{-0.11}$	$2.51^{+0.49}_{-0.55}$
VVDS-02h	[0.7−0.9]	1398	−19.20	1.36	$2.87^{+0.51}_{-0.52}$	$1.72^{+0.19}_{-0.12}$	$2.87^{+0.50}_{-0.52}$
VVDS-02h	[0.9−1.1]	1025	−19.66	1.35	$2.87^{+0.62}_{-0.66}$	$1.77^{+0.24}_{-0.14}$	$2.75^{+0.60}_{-0.63}$
VVDS-02h	[1.1−1.3]	561	−20.26	1.35	$3.09^{+0.61}_{-0.65}$	$1.96^{+0.27}_{-0.21}$	$2.93^{+0.58}_{-0.62}$
VVDS-02h	[1.3−2.1]	432	−20.93	1.25	$3.63^{+0.63}_{-0.76}$	$1.92^{+0.31}_{-0.31}$	$3.69^{+0.77}_{-1.00}$
VVDS-02h"DEEP2" selection	[0.7−1.35]	1620	−20.00	1.36	$3.05^{+0.51}_{-0.53}$	$1.56^{+0.14}_{-0.11}$	$3.17^{+0.53}_{-0.55}$
VVDS-02h"DEEP2" selection	[0.7 − 0.9]	687	−19.65	1.41	$3.59^{+0.77}_{-0.83}$	$1.65^{+0.25}_{-0.17}$	$3.59^{+0.77}_{-0.83}$
VVDS-02h"DEEP2" selection	[0.9−1.35]	933	−20.25	1.32	$3.29^{+0.57}_{-0.59}$	$1.82^{+0.19}_{-0.15}$	$3.13^{+0.54}_{-0.57}$
VVDS-CDFS	[0.4−0.7]	421	−19.44	1.30	$3.19^{+0.93}_{-1.01}$	$1.45^{+0.25}_{-0.17}$	$3.31^{+1.06}_{-1.26}$
VVDS-CDFS	[0.6−0.8]	372	−19.74	1.47	$4.55^{+1.25}_{-1.46}$	$1.48^{+0.28}_{-0.15}$	$4.15^{+1.25}_{-1.50}$
VVDS-CDFS	[0.8−1.5]	452	−20.43	1.34	$3.53^{+1.29}_{-1.66}$	$1.66^{+0.40}_{-0.27}$	$3.49^{+1.28}_{-1.78}$

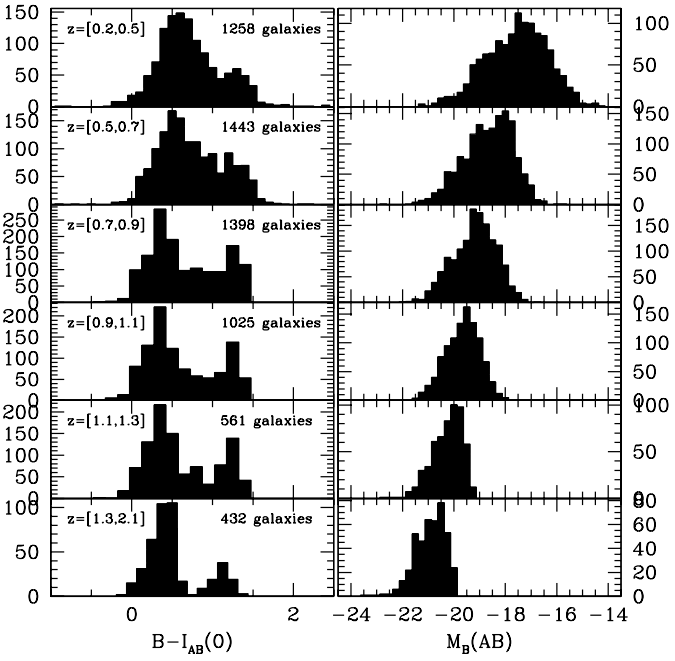

Fig. 2. The rest frame $B-I_{AB}$ color (*left*) and absolute magnitude $M_{B_{AB}}$ (*right*) from the VVDS-02h data up to $z \sim 2$.

3.1. Estimating correlation functions from the VVDS

To measure the galaxy real-space correlation length r_0 and slope γ from our survey, we have used the projection of the bi-dimensional correlation function $\xi(r_{\rm p}, \pi)$. This function was estimated using the well-known Landy & Szalay (1993) estimator

$$\xi(r_{\rm p}, \pi) = \frac{N_{\rm R}(N_{\rm R}-1)}{N_{\rm G}(N_{\rm G}-1)} \frac{GG(r_{\rm p}, \pi)}{RR(r_{\rm p}, \pi)} - 2\frac{N_{\rm R}-1}{N_{\rm G}} \frac{GR(r_{\rm p}, \pi)}{RR(r_{\rm p}, \pi)} + 1 \quad (1)$$

where $N_{\rm G}$ is the mean galaxy density (or, equivalently, the total number of objects) in the survey; $N_{\rm R}$ is the mean density of a catalogue of random points distributed within the same volume of the considered redshift bin; $GG(r)$ is the number of independent galaxy-galaxy pairs with separation between r and $r + {\rm d}r$; $RR(r)$ is the number of independent random-random pairs and $GR(r)$ the number of cross galaxy-random pairs within the same interval of separations. A total of ∼40 000 random points have been used in each redshift bin, guaranteeing a sufficient density to avoid shot-noise effects on small scales. The random sample follows exactly the same geometry, redshift distribution and observational pattern as in the galaxy data, while a specific weighting scheme is used to overcome the biases introduced by the slit-positioning software and other selection effects. These techniques have been extensively tested on a large number of mock VVDS surveys and have been shown to be able to recover the correct $w_{\rm p}(r_{\rm p})$ correlation function to better than 10%, reducing any systematic effect to less than 5%. We have not applied this small correction to the data presented in this paper. This is discussed in detail in the accompanying paper by Pollo et al. (2005).

Since we are not computing the correlation function from the full magnitude-limited survey altogether, there is no point here in using the so-called J_3 minimum-variance weighting. This usually has been adopted in the analysis of large flux-limited local surveys (Fisher et al. 1994; Guzzo et al. 2000),

in which the sampling of the clustering process varies dramatically between the nearby and distant parts of the sample. Its main scope is to avoid excessive weighting of the most distant parts of the sample, where only sparse bright galaxies trace structures. Within each of our redshift bins, the density of objects varies only slightly and equal weighting of the pairs is the most appropriate choice (Fisher et al. 1994).

3.2. $\xi(r_p, \pi)$, $w_p(r_p)$ and the correlation length r_0

We have computed the two point correlation function $\xi(r_p, \pi)$ in increasing redshift bins, selecting the bin boundaries to maximize the number of objects, hence the signal to noise of the correlation function, in each of the bins.

The formalism developed by Davis & Peebles (1983) has been used to derive the real space correlation function in the presence of redshift-space distortions along the line of sight. We integrate $\xi(r_p, \pi)$ along the line of sight, computing

$$w_p(r_p) \equiv 2 \int_0^\infty dy \xi(r_p, \pi) = 2 \int_0^\infty dy \xi \left[\left(r_p^2 + y^2 \right)^{1/2} \right], \quad (2)$$

where in practice the upper integration limit has to be chosen finite, to avoid adding noise to the result. After a few experiments, we used a value of 20 h^{-1} Mpc.

If we assume a power-law form for $\xi(r)$, i.e.

$$\xi(r) = \left(\frac{r}{r_0} \right)^{-\gamma}, \quad (3)$$

$w_p(r_p)$ can be written as

$$w_p(r_p) = r_p \left(\frac{r_0}{r_p} \right)^\gamma \frac{\Gamma\left(\frac{1}{2}\right) \Gamma\left(\frac{\gamma-1}{2}\right)}{\Gamma\left(\frac{\gamma}{2}\right)}, \quad (4)$$

where Γ is the Euler Gamma function.

Fitting the $w_p(r_p)$ measurements in each redshift bin then provides a measurement of $r_0(z)$ and $\gamma(z)$.

3.3. Computing errors

The uncertainty associated with the computation of $r_0(z)$ and $\gamma(z)$ is largely dominated by cosmic variance. Although our spectroscopic sample is the largest available to date at the redshifts probed, both in the number of galaxies and area surveyed, only two fields have been sampled, with the VVDS-02h largely dominating over the VVDS-CDFS in terms of the number of galaxies observed and area covered, and it is therefore inappropriate to estimate errors on $w_p(r_p)$, $r_0(z)$, and $\gamma(z)$ directly from field-to-field variations within our data set. Instead, we have been using ensemble errors derived from the scatter in the correlation function computed from 50 mock VVDS surveys constructed using the GalICS simulations (Blaizot et al. 2005), as thoroughly described in the parallel paper by (Pollo et al. 2005). These realistic mock samples specifically include the same selection function and observational biases present in the VVDS First Epoch data set, and allow us to compute ensemble statistical averages and scatters of the quantities we measure on the real data. In particular, the standard deviation of the measured $w_p(r_p)$ from the mock VVDS samples provides us with a realistic set of error bars that include also the effect of field-to-field variations due to fluctuations on scales larger than the observed field, i.e. cosmic variance (obviously assuming that the λ-CDM power spectrum and normalization are a good match to the observed one, which is indeed the case).

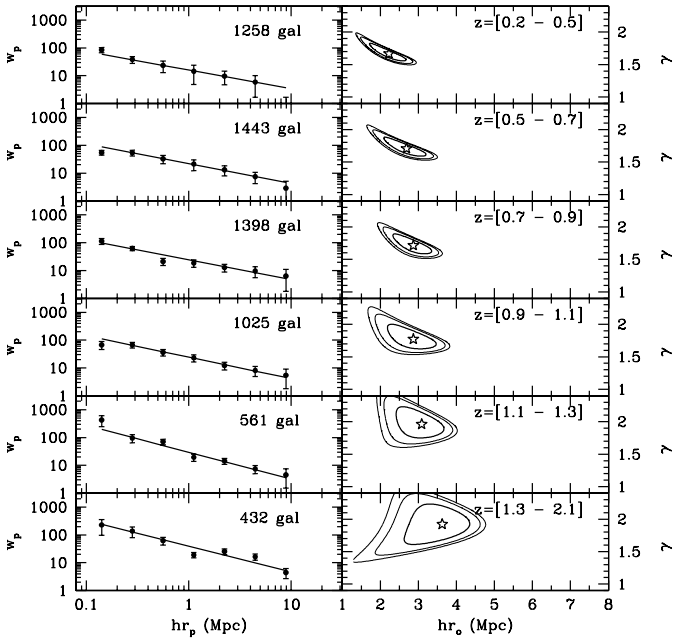

Fig. 3. The correlation function from the VVDS-02h data up to $z \simeq 2$: (*left*) $w_p(r_p)$ measured in 6 redshift bins, the number of galaxies in each bin is indicated on the top right of each panel, (*right*) the correlation length $r_0(z)$ and correlation function slope γ measured from fitting $w_p(r_p)$ assuming a power law form $\xi(r) = (r/r_0)^{-\gamma}$. 68%, 90% and 95% likelihood contours are drawn.

The comparison of the VVDS-02h and VVDS-CDFS correlation functions gives us an external check to this procedure, with a relatively noisy indication of the amplitude of cosmic variance, as described below.

4. Results

4.1. The VVDS correlation function from a magnitude limited sample $17.5 \leq I_{AB} \leq 24$ out to $z \simeq 2$

We have computed the correlation function $\xi(r_p, \pi)$ and its projection $w_p(r_p)$ on both the VVDS-02h and VVDS-CDFS fields.

The correlation function $w_p(r_p)$ is presented in the left panel of Fig. 3 for the VVDS-02h field, and in Fig. 4 for the VVDS-CDFS field. The number of galaxies observed in each field is indicated for each redshift bin in Fig. 3, so far the largest sample of galaxies used to compute the correlation function at these redshifts. The large sample allows to compute $w_p(r_p)$ in 6 redshift bins up to $z = 2.1$ for the VVDS-02h field, and in 3 bins up to $z = 1.5$ for the VVDS-CDFS field. Error bars are ensemble errors computed as described in Sect. 3.3. A positive correlation signal is measured out to at least 30 h^{-1} Mpc in all bins, and $w_p(r_p)$ is well described by a power law in the range $0.1 \leq r_p \leq 10$ h^{-1} Mpc (note however that any redshift space

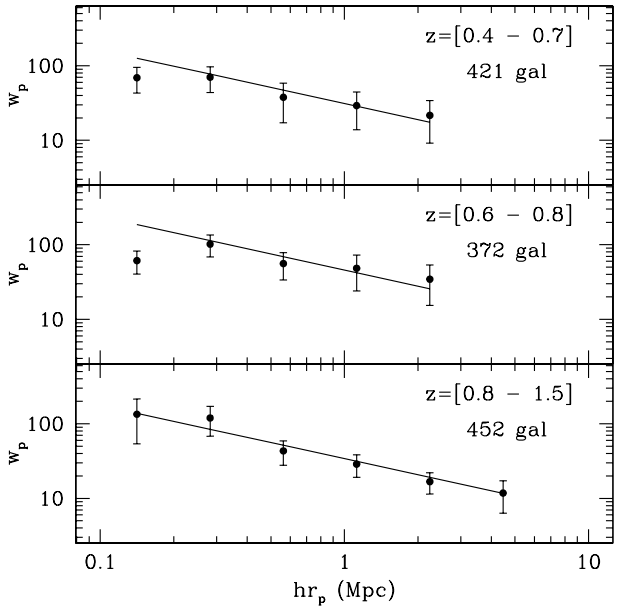

Fig. 4. The correlation function $w_p(r_p)$ for the VVDS-CDFS data in three redshift bins from $z = 0.4$ to to $z = 1.5$. The slope has been fixed to $\gamma = 1.72$, i.e. the mean measured in the VVDS-02h field in the range $z = [0.2,\ 1.1]$.

feature in $\xi(r)$ is smoothed out in $w_p(r_p)$, which is its integral). The measured correlation function amplitude is relatively low at low redshifts $z \leq 0.5$, and stays essentially constant as a function of redshift, with just a mild increase in the farthest bins. A possible interpretation of these results is discussed in the next sections.

4.2. Evolution of the galaxy real-space correlation function

The measured values of the correlation length $r_0(z)$ and the correlation function slope $\gamma(z)$ computed from the fitting of $w_p(r_p)$ are reported in Table 1. For the VVDS-02h field, we have used all w_p points for $0.1 \leq r_p \leq 10\ h^{-1}$ Mpc. For the VVDS-CDFS field, we have used points in the range $0.1 \leq r_p \leq 3\ h^{-1}$ Mpc only, because of the smaller field size. We also report in Table 1 the values of $r_0(z)$ obtained after fitting w_p with the slope γ fixed to the average slope measured in the range $z = [0.2,\ 1.3]$. In the VVDS-CDFS, a strong wall-like large scale structure has been identified at $z \sim 0.735$, with more than 130 galaxies in a velocity range ± 2000 km s^{-1} (Le Fèvre et al. 2004b), and is expected to strongly affect the correlation function computation. The correlation function in this field has been computed in the redshift interval $z = [0.6,\ 0.8]$ which includes this strong structure, as well as in $z = [0.4,\ 0.7]$ and $z = [0.8,\ 1.5]$ to specifically exclude it, as reported in Table 1. While we find a slightly higher correlation length in the VVDS-CDFS, the measurements are compatible, within the errors, with the values reported for the VVDS-02h.

We have investigated how our results change when using the full set of available redshifts, i.e. including also the 1300 less accurate measurements (flag 1), which are shown to be ∼55% correct (Le Fèvre et al. 2005). The result is that the measured correlation lengths are lowered by ∼3−5%, which we interpret as a consequence of the significant fraction of poorly measured redshifts which dilute the actual correlation function.

The results strikingly show a slowly increasing correlation length over the complete redshift range $z = [0.2,\ 2.1]$. The lowest value measured is in the lowest redshift bin probed, then r_0 is constant $r_0 \sim 2.8\ h^{-1}$ Mpc over the range $z = [0.5,\ 1.1]$ and increases slightly to $r_0 \sim 3.6\ h^{-1}$ Mpc over $z = [1.1,\ 2.1]$. When we fit the slope γ of the correlation function at the same time as r_0, it varies between 1.67 and 1.96, slightly increasing with redshift, as reported in Table 1. The average slope in the range $z = [0.2,\ 1.3]$ is $\gamma = 1.76$.

4.3. Comparison with other surveys

In redshift surveys of the local Universe ($z < 0.2$), the lowest values for the correlation length have been measured for late-type star forming galaxies as e.g. H-II galaxies ($r_0 = 2.7\ h^{-1}$ Mpc, Iovino et al. 1988) and infrared-selected *IRAS* galaxies ($r_0 = 3.76\ h^{-1}$ Mpc, Fisher et al. 1994). Here we measure an even lower correlation length for galaxies with $z = [0.2,\ 0.5]$ in the VVDS, coherent with their very low intrinsic luminosity as discussed in Sect. 5.

In order to compare our measurements at higher redshifts to the measurements of the DEEP2 survey (Coil et al. 2004), we have restricted our data by applying a-posteriori the same color and magnitude selection function as the DEEP2 survey applied a-priori to pre-select its spectroscopic targets in the redshift range 0.7−1.35. With this "DEEP2" selection function ($R_{AB} \leq 24.1$, $B - R \leq 2.35(R - I) - 0.45$, $R - I \geq 1.15$ or $B - R \leq 0.5$) only 59% of the VVDS I-band magnitude-limited sample galaxies are selected (in the desired redshift range). The correlation function $w_p(r_p)$, and the corresponding $r_0(z)$ and $\gamma(z)$ of this sample are shown in Fig. 5. We find that $r_0 = 3.51 \pm 0.63\ h^{-1}$ Mpc for the full $z = [0.7,\ 1.35]$ sample, compared to 3.19 ± 0.51 by Coil et al. (2004). Separating in the same redshift bins, and setting the slope to $\gamma = 1.66$ as measured in DEEP2, we find that $r_0 = 3.37 \pm 0.67\ h^{-1}$ Mpc in $z = [0.7,\ 0.9]$, $r_0 = 3.05 \pm 0.47\ h^{-1}$ Mpc in $z = [0.9,\ 1.35]$, while Coil et al. (2004) find $r_0 = 3.53 \pm 0.81\ h^{-1}$ Mpc and $r_0 = 3.12 \pm 0.72\ h^{-1}$ Mpc, respectively, as shown in Fig. 6. Given the relative uncertainties of both surveys, these results are therefore in excellent agreement. The correlation function for the DEEP2 survey therefore differs from the correlation function of the complete VVDS sample because of the different selection function applied that selects galaxies brighter than in the VVDS and excludes galaxies relatively blue in $R - I$ ($R - I < 0.7$) but still red in $B - R$ ($B - R > 0.6$), resulting in a larger correlation length.

5. Discussion: evolution of the clustering length $r_0(z)$ from $z \simeq 2$

The evolution of the clustering length $r_0(z)$ from the VVDS first epoch "Deep" sample of galaxies with $17.5 \leq I_{AB} \leq 24$ is presented in Fig. 7. The redshift of each bin is computed as the mean of the redshifts of galaxies in each bin. We find that r_0 is roughly constant or possibly slightly increasing,

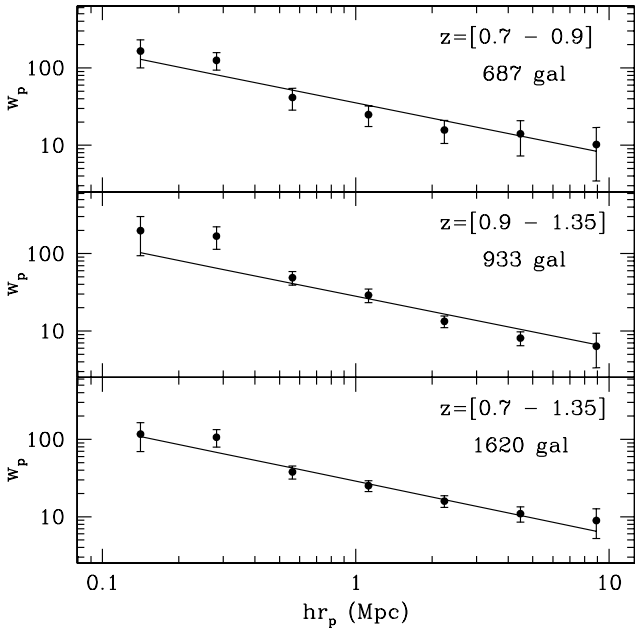

Fig. 5. Correlation function computed from the VVDS sample, applying the same color–magnitude selection function as for the DEEP2 survey (Coil et al. 2004): (*bottom*) the full sample in the redshift range [0.7, 1.35], (*top two panels*) the lower [0.7, 0.9] and higher [0.9, 1.35] redshift samples. The slope has been fixed to the same slope as measured in the DEEP2 to ease r_0 comparison.

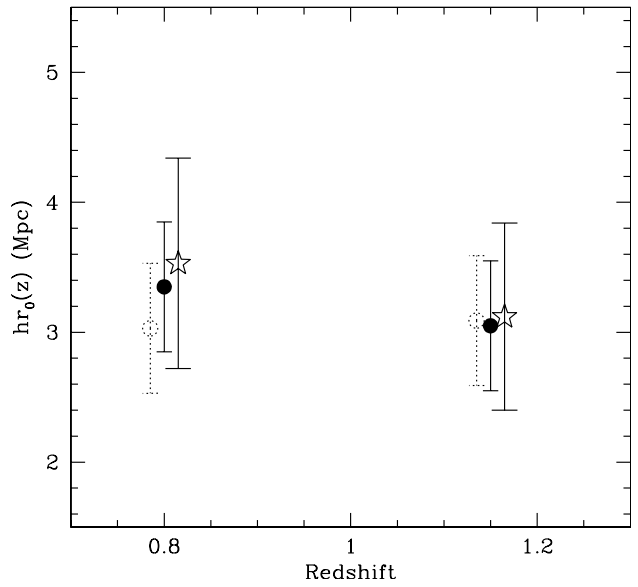

Fig. 6. Comparison of the correlation length $r_0(z)$ (comoving) measured in the VVDS-Deep survey applying a color-color and magnitude selection as in the DEEP2 survey, and the DEEP2 survey measurements (Coil et al. 2004): VVDS-02h, with $\gamma = 1.66$ fixed to the DEEP2 value: filled circles; r_0 and γ fitted simultaneously: open-dot circles, DEEP2 measurements: open stars. Data points have been shifted slightly along the redshift axis to avoid overlap.

within our measurement errors, as redshift increases, with a low value of $r_0 = 2.35^{+0.36}_{-0.37}\ h^{-1}$ Mpc for $z = [0.2, 0.5]$, to $r_0 = 3.03^{+0.51}_{-0.56}\ h^{-1}$ Mpc for $z = [1.3, 2.1]$.

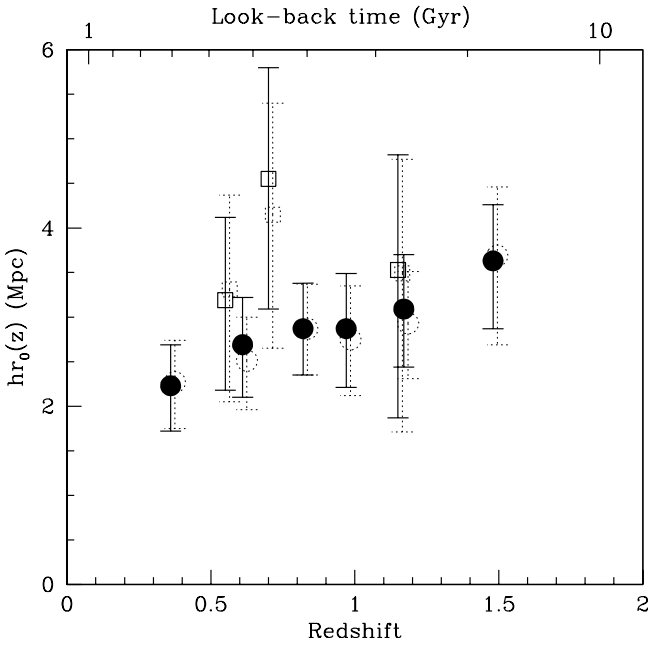

Fig. 7. Evolution of the correlation length $r_0(z)$ (comoving) from the VVDS. Black circles are for the VVDS-02h data, open squares are for the VVDS-CDFS data. The doted points indicate the measurements when setting the slope to the mean $\gamma = 1.76$ measured in the range $z = [0.2,\ 1.3]$. Associated errors have been computed from the fitting of $w_p(r_p)$ and associated errors drived from 50 mock galaxy samples from Galics (see text). The VVDS-CDFS measurements are slightly higher than in the VVDS-02h, but remain compatible within the measurement errors. The VVDS-CDFS measurement at $z = 0.7$ include a strong over-density of more than 130 galaxies (see Le Fèvre et al. 2004b), making the correlation function higher in this bin.

Ideally, one would like to follow the evolution of the clustering of the mass in the universe, translated into the gravitational growth of structures. To access to this measurement from the correlation length of galaxies requires understanding of the evolution of galaxies as complex physical systems, and to be able to relate the populations of galaxies observed at different redshifts as descendents of a well-identified original population of matter halos at early epochs. Although the VVDS I-band magnitude selection is the minimum selection bias one can impose selecting a distant sample, this faint magnitude limit leads to a broad redshift coverage, and to a population mix in the VVDS sample that changes with redshift as described in Sect. 2.2. Over the redshift range considered here, the luminosity function of galaxies in the VVDS is strongly evolving up to ∼1.5−2 mag (Ilbert et al. 2005). The interpretation of the evolution of $r_0(z)$ is therefore not direct.

In the lower redshift bin $z \leq 0.5$, we find a correlation length smaller than any other population of galaxies observed today. The mean absolute luminosity of the low redshift sample is $M_{B_{AB}} = -17.5$ with a significant number of objects fainter than $M_{B_{AB}} = -16$ (Fig. 2), while bright galaxies are under-represented due to the small volume available at these low redshifts. Not surprisingly given the faint $I_{AB} = 24$ cut-off in the VVDS, this makes it the faintest galaxy population for which 3D clustering has ever been probed at low redshifts, about 1.5 mag fainter than the 2dFGRS sample with a mean

$M_{b_J} = -17.98$ equivalent to $M_{B_{AB}} = -18.9$ (Norberg et al. 2001). This low clustering of the low luminosity population of galaxies measured in the VVDS is roughly consistent with an extrapolation to fainter luminosities of the trend for a lower correlation length as galaxies become fainter, as observed locally in the 2dFGRS and SDSS surveys (Norberg et al. 2001; Zehavi et al. 2002), and at intermediate redshifts in the CNOC2 survey (Shepherd et al. 2001).

As redshift increases, the VVDS probes more of the bulk of the general population of galaxies. Galaxies sampled at redshifts 0.5−1.1 become increasingly similar in luminosity and color to the population sampled by the low redshift 2dFGRS and SDSS surveys. As can be seen from Fig. 2, at $z \simeq 1$ we measure the clustering of galaxies with a mean absolute magnitude $M_{B_{AB}} = -18.5$, after taking into account ∼1 mag of luminosity brightening at $z \simeq 1$ (Ilbert et al. 2005), thus comparable to the bulk of the galaxies probed by 2dF and SDSS at $z \simeq 0.1$.

Over the redshift range $z = [0.5,\ 1.1]$, we find a slightly increasing correlation length $r_0 \simeq 2.2$–$2.9\ h^{-1}$ Mpc. For a similar, blue-selected, population of galaxies at $z \simeq 0.15$, the 2dFGRS finds $r_0 \simeq 4.3$–$4.6\ h^{-1}$ Mpc (Norberg et al. 2001), using the same technique we use here. Note that at a redshift similar to the 2dFGRS, the SDSS tends to sample a different mix of morphological types, due to its red-based selection, and for this reason measures a larger correlation length, $r_0 = 6.14 \pm 0.18\ h^{-1}$ Mpc (Zehavi et al. 2002; see Hawkins et al. 2003, for discussion). Our results therefore seem to indicate that the amplitude of the correlation function of galaxies which would have luminosities $M_{B_{AB}} = -19.5$ after correction for luminosity evolution is about 2.5 times lower at $z = 1$ than observed locally by the 2dFGRS.

While we know that galaxies with similar luminosities at different redshifts may not be tracing the underlying dark matter in a similar way (see Marinoni et al. 2005), this result is in qualitative agreement with the expectations of the simple gravitational growth of primordial fluctuations (see e.g. Fig. 5 of Weinberg et al. 2004).

In the highest redshift bins $z = [1.1,\ 1.3]$ and $z = [1.3,\ 2.1]$, we are measuring the correlation function of the brightest $M_{B_{AB}} \leq -19.5$ galaxies, with a mean of $M_{B_{AB}} \sim -20.5$ and ∼−21.0 respectively. We observe that the correlation length increases compared to the measurements in the range $z = [0.5,\ 1.1]$, up to $r_0 \simeq 3\ h^{-1}$ Mpc at $z = 1.2$ and $r_0 \simeq 3.6\ h^{-1}$ Mpc in the highest redshift bin to $z \simeq 2$. The luminosity function of galaxies at these redshifts shows a marked evolution, equivalent to an increase in luminosity of ∼1.5 and ∼2 mag in $z = [1.1,\ 1.3]$ and $z = [1.3,\ 2.1]$, respectively (Ilbert et al. 2005). These galaxies will therefore be expected to have a mean $M_{B_{AB}} \sim -19.5$ at low redshifts after evolution. Again, comparing the clustering observed in the VVDS to the clustering length of $r_0 \simeq 5\ h^{-1}$ Mpc measured for $M_{B_{AB}} = -19.5$ in the 2dFGRS (Norberg et al. 2001), we find that the clustering amplitude has increased by a factor ≃2.4 from $z \sim 1.3$–1.5 to $z = 0$.

The evolution of the correlation length observed in our data is in broad agreement with the results of computer simulations of galaxy formation and evolution. In their SPH simulation, Weinberg et al. (2004) find that the clustering length of galaxies decreases from $r_0 \sim 4.2\ h^{-1}$ Mpc at $z = 3$ to a minimum $r_0 \sim 3.0\ h^{-1}$ Mpc at $z = 1.5$, then increases again to $r_0 \sim 4.0\ h^{-1}$ Mpc at $z = 1$. Note, however, that these predictions refer to the correlation length of the same class of galaxies, corresponding to $M > 5 \times 10^{10}\ M_\odot$, ideally followed at different redshifts. In a real, magnitude-limited observation, as we have discussed, this effect is related to the different range of luminosities sampled at each redshift, and the changing clustering strength at different luminosities. Besides the simulated clustering of galaxies, the dark matter correlation length is expected from theory and N-body simulations to drop steeply with increasing redshift, from $r_0 \sim 5\ h^{-1}$ Mpc at $z = 0$ to $r_0 \sim 1.8\ h^{-1}$ Mpc at $z = 1.5$ (see e.g. Weinberg et al. 2004). In comparison to these predictions, our data clearly show that the clustering evolution of galaxies does not follow the predicted trend for dark matter.

6. Conclusions

We have computed the evolution of the correlation function $\xi(r_\mathrm{p}, \pi)$ and its integral along the line of sight $w_\mathrm{p}(r_\mathrm{p})$, from the VVDS first epoch "deep" survey. The VVDS contains a large spectroscopically-selected sample of 7155 galaxies representative of the global galaxy population in the redshift range $z = [0,\ 2.1]$, in a large $0.61\mathrm{deg}^2$ total area. The correlation length r_0 is observed to be low, $r_0 \simeq 2.2\ h^{-1}$ Mpc, for the low redshift $z \leq 0.5$ population, indicating the low clustering of the very low luminosity population sampled in this redshift range. Over the redshift range $z = [0.5,\ 1.1]$, the correlation length of the population of galaxies, with a luminosity range comparable to the lower redshift 2dFGRS and SDSS, stays roughly constant with $r_0 \simeq 2.8\ h^{-1}$ Mpc. At the highest redshifts probed in this paper, $z = [1.1,\ 2.1]$, we find that the correlation length increases slightly to $r_0 \simeq 3.6\ h^{-1}$ Mpc.

After applying the same selection function as in the DEEP2 survey, our results are found to be in excellent agreement with the results of Coil et al. (2004). However, the significantly different DEEP2 selection function excludes up to 41% of the galaxy population observed by the VVDS, making the correlation length of the DEEP2 sample larger than in the purely magnitude-selected VVDS. The VVDS results demonstrate that the clustering of the whole galaxy population at the same redshift is indeed significantly lower, with $r_0 \simeq 2.9$ in the VVDS vs. $r_0 \simeq 3.5\ h^{-1}$ Mpc in the DEEP2, further emphasizing the importance of our simple, purely magnitude-limited selection function.

Our measurements clearly show that the correlation length evolves only slowly with redshift in the range $0.5 \leq z \leq 2$, in a magnitude limited sample with $17.5 \leq I_{AB} \leq 24$. Taking into account the different VVDS galaxy populations probed as a function of redshift, with intrinsically brighter galaxies probed as redshift increases, we find that the clustering of galaxies at $z \sim 1$–2 in the VVDS is about 2.5 times lower in amplitude than for the galaxies probed by the 2dFGRS at $z \sim 0.15$, for populations with similar absolute M_B magnitudes. This result provides unambiguous evidence for clustering evolution.

Our results are in broad agreement with simulations accounting for both gravitational growth and baryonic physics

(Weinberg et al. 2004; Benson et al. 2001). These simulations show that the underlying dark matter correlation evolves strongly with redshift, as expected in a hierarchical growth of structures. Our observation that the clustering of galaxies does not follow such a strong evolution therefore fully supports the model in which luminous galaxies at $z = 1-2$ (or 9−10 billion years ago) trace the emerging peaks of the large-scale dark-matter distribution and implies a strongly evolving galaxy bias.

We will investigate the evolution of the galaxy – dark matter bias elsewhere (Marinoni et al. 2005). A more detailed study of the dependance of clustering on luminosity and galaxy type will be presented in forthcoming papers.

Acknowledgements. This research has been developed within the framework of the VVDS consortium (formerlly VIRMOS consortium).
This work has been partially supported by the CNRS-INSU and its Programme National de Cosmologie (France), and by Italian Research Ministry (MIUR) grants COFIN2000 (MM02037133) and COFIN2003 (No. 2003020150).
The VLT-VIMOS observations have been carried out on guaranteed time (GTO) allocated by the European Southern Observatory (ESO) to the VIRMOS consortium, under a contractual agreement between the Centre National de la Recherche Scientifique of France, heading a consortium of French and Italian institutes, and ESO, to design, manufacture and test the VIMOS instrument.

References

Benoist, C., Maurogordato, S., da Costa, L. N., Cappi, A., & Schaeffer, R. 1996, ApJ, 472, 452
Benson, A. J., Frenk, C. S., Baugh, C. M., Cole, S., & Lacey, C. G. 2001, MNRAS, 327, 1041
Blaizot, J., Wadadekar, Y., Guiderdoni, B., et al. 2005, MNRAS, 360, 159
Cabanac, R. A., de Lapparent, V., & Hickson, P. 2000, A&A, 364, 349
Carlberg, R., Yee, H. K. C., Morris, S. L., et al. 1999, Phil. Trans. R. Soc. Lond. A, 357, 167
Coil, A. L., Davis, M., Madgwick, D. S., et al. 2004, ApJ, in press
Colless, M. M., Dalton, G., Maddox, S., et al. 2001, MNRAS, 328, 1039
Davis, M., & Peebles, P. J. E. 1983, ApJ, 267, 465
Fisher, K. B., Davis, M., Strauss, M. A., Giovanelli, R., & Haynes, M. P. 1994, MNRAS, 266, 50
Foucaud, S., McCracken, H. J., Le Fèvre, O., et al. 2003, A&A, 409, 835
Giacconi, R., Zirm, A., Wang, J., et al. 2002, ApJS, 139, 369
Giavalisco, M., Steidel, C. C., Adelberger, K. L., et al. 1998, ApJ, 503, 543
Giovanelli, R., Haynes, M. P., & Chincarini, G. 1986, ApJ, 300, 77
Governato, F., Baugh, C. M., Frenk, C. S., et al. 1998, Nature, 392, 359
Guzzo, L., Iovino, A., Chincarini, G., Giovanelli, R., & Haynes, M. P. 1991, ApJ, 382, L5
Guzzo, L., Strauss, M. A., Fisher, K. B., Giovanelli, R., & Haynes 1997, ApJ, 489, 37
Guzzo, L., Bartlett, J. G., Cappi, A., et al. 2000, AA, 355, 1
Hawkins, E., Maddox, S., Cole, S., et al. (2dF Team) 2003, MNRAS, 346, 78
Ilbert, O., Tresse, L., Zucca, E., and the VVDS consortium 2005, A&A, 439, 863
Iovino, A., Melnick, J., & Shaver, P. 1988, ApJ, 330, L17
Kauffmann, G., Colberg, J. M., Diaferio, A., & White, S. D. M. 1999, MNRAS, 303, 188
Landy, S. D., & Szalay, A. S. 1993, ApJ, 412, 64
Le Fèvre, O., Hudon, D., Lilly, S. J., et al. 1996, ApJ, 461, 534
Le Fèvre, O., and the VVDS consortium 2003, The Messenger 111, 18
Le Fèvre, O., Mellier, Y., McCracken, H. J., et al. 2004a, A&A, 417, 839
Le Fèvre, O., and the VVDS consortium 2004b, A&A, 428, 1043
Le Fèvre, O., Vettolani, G., Garilli, B., and the VVDS consortium 2005, A&A, 439, 845
Lilly, S. J., Le Fèvre, O., Crampton, D., Hammer, F., & Tresse, L. 1995, ApJ, 455, 50
McCracken, H. J., Le Fèvre, O., Brodwin, M., et al. 2001, A&A, 376, 756
McCracken, H. J., Radovich, M., Bertin, E., et al. 2003, A&A, 410, 17
Marinoni, C., Le Fèvre, O., Meneux, B., and the VVDS consortium, A&A, submitted
Norberg, P., Baugh, C. M., Hawkins, E., et al. 2001, MNRAS, 328, 64
Norberg, P., Baugh, C. M., Hawkins, E., et al. 2002, MNRAS, 332, 827
Pollo, A., Meneux, B., Guzzo, L., and the VVDS consortium 2005, A&A, 439, 887
Peacock, J. 2002, Tenerife Winter School, Dark matter and dark energy in the universe [arXiv:astro-ph/0309240]
Postman, M., Lauer, T. R., Szapudi, I., & Oegerle, W. 1998, ApJ, 506, 33
Roche, N., & Eales, S. A. 1999, MNRAS, 307, 703
Shepherd, C. W., Carlberg, R. G., Yee, H. K. C., et al. 2001, ApJ, 560, 72
Small, T. A., Ma, C., Sargent, W. L. W., & Hamilton, D. 1999, ApJ, 524, 31
Somerville, R. S., Lemson, G., Sigad, Y., et al. 2001, MNRAS, 320, 289
Schneider, D. P., Fan, X., Hall, P. B., et al. 2003, AJ, 126, 2579
Steidel, C. C., Adelberger, K. L., Dickinson, M., et al. 1998, ApJ, 492, 428
Weinberg, D. H., Davé, R., Katz, N., & Hernquist, L. 2004, ApJ, 601, 1
Zehavi, I., Blanton, M. R., Frieman, J. A., et al. 2002, ApJ, 571, 172
Zehavi, I., Weinberg, D. H., Zheng, Z., et al. 2004, ApJ, 608, 16